

Experimental demonstration of a dusty plasma ratchet rectification and its reversal

Ya-feng He^{1,*}, Bao-quan Ai^{2,†}, Chao-xing Dai¹, Chao Song¹,
Rui-qi Wang¹, Wen-tao Sun¹, Fu-cheng Liu¹, and Yan Feng^{3,‡}

¹*Hebei Key Laboratory of Optic-electronic Information Materials,
College of Physics Science and Technology, Hebei University, Baoding 071002, China*

²*Guangdong Key Laboratory of Quantum Engineering and Quantum Materials,
SPTE, South China Normal University, Guangzhou 510006, China*

³*Center for Soft Condensed Matter Physics and Interdisciplinary Research,
School of Physical Science and Technology, Soochow University, Suzhou 215006, China.*

(Dated: December 21, 2024)

The naturally persistent flow of hundreds of dust particles is experimentally achieved in a dusty plasma system with the asymmetric sawteeth of gears on the electrode. It has also demonstrated that the direction of the dust particle flow can be controlled by changing the plasma conditions of the gas pressure or the plasma power. Numerical simulations of dust particles verify the experimental observations of the flow rectification of dust particles. Both experiments and simulations suggest that the asymmetric electric potential and the collective effect are two keys in this dusty plasma ratchet.

A dusty plasma (or complex plasma) consists of micron-sized dust particles immersed in plasma environments such as the ionosphere, the semiconductor manufacture and the laboratory [1, 2]. These dust particles are highly charged so that they can be strongly coupled [3–16]. Due to the various heating mechanisms in plasmas, such as the plasma instability [17] and the spatial/temporal particle charge fluctuation, the kinetic energy of these dust particles can reach from several eV [10] to tens eV [18, 19] or even higher. Realizing the manipulation of those energetic dust particles can lead to further scientific insights and applications such as the particle separation and the energy collection. Turning the random motion of these dust particles into the directional motion will definitely pave the way for this manipulation. The Feynman ratchet model provides a strategy to rectify the nonequilibrium fluctuations into the directional motion of particles [20, 21]. Here, we demonstrate a dusty plasma ratchet to experimentally realize a rectification of dust particles in a radio-frequency (rf) plasma, i.e., the dust particles are rectified into a directional flow by the Feynman ratchet strategy. Remarkably, we can experimentally control the direction of particle flow by regulating the gas pressure or the rf power of the plasma. We further explore the rectification mechanisms of the dusty plasma ratchet by performing numerical simulations.

Experiments. –A circular resin gear (named inner gear) with asymmetric sawtooth is placed concentrically with another circular resin gear (named outer gear) on a horizontal lower electrode, as shown in Fig. 1(a). The sizes of the inner and outer gears are 9 mm in height, 11.75 and 23 mm in radius, 1.5 and 4 mm in depth, respectively

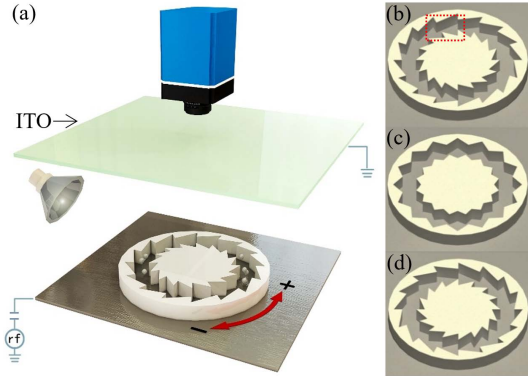


FIG. 1. (color online). Sketch of the dusty plasma ratchet experiment (a). Dust particles can perform a specific directional motion along the saw channel enclosed by the inner and outer gears. Here, we define the positive and negative motion directions as ‘+’ and ‘-’ shown. (b)–(d) show gears with different orientation on the sawtooth. The asymmetric orientation on the sawtooth in (b) is opposite to that in (d). In (c), the sawtooth is symmetrical along the saw channel. The field of view in our data analysis is marked by using a dotted rectangle in (b). Dust particles suspend at $\sim 5 - 9$ mm above the lower electrode at different conditions. ITO: Indium Tin Oxides glass plate.

[22]. The orientation of the sawtooth in the inner gear is the same as that in the outer gear, so that the inner and outer gears enclose a saw channel. As a result, the width of the enclosed saw channel changes periodically.

Argon plasma is produced in a vacuum chamber by coupling capacitively the lower electrode to a radio-frequency power source (13.56 MHz) via a capacitor. Then, we introduce macroporous crosslinked polystyrene microspheres (dust particles) into one side of the saw channel by using a capillary glass tube. The radius of each dust particle is $r_d = 11.5 \mu\text{m}$ and the mass density is $\sim 0.7 \text{ g/cm}^3$ as reported by the manufacturer. In the

* Email:heyf@hbu.edu.cn

† Email:aibq@scnu.edu.cn

‡ Email:fengyan@suda.edu.cn

plasma, these dust particles are negatively charged immediately, and flow along the saw channel until they fill up the channel due to the Coulomb repulsion. They are illuminated by a 18 W flood lamp from side and imaged by a camera from the upper transparent electrode. After the motion of dust particles is recorded, we use the moment method [23] to calculate positions of dust particles.

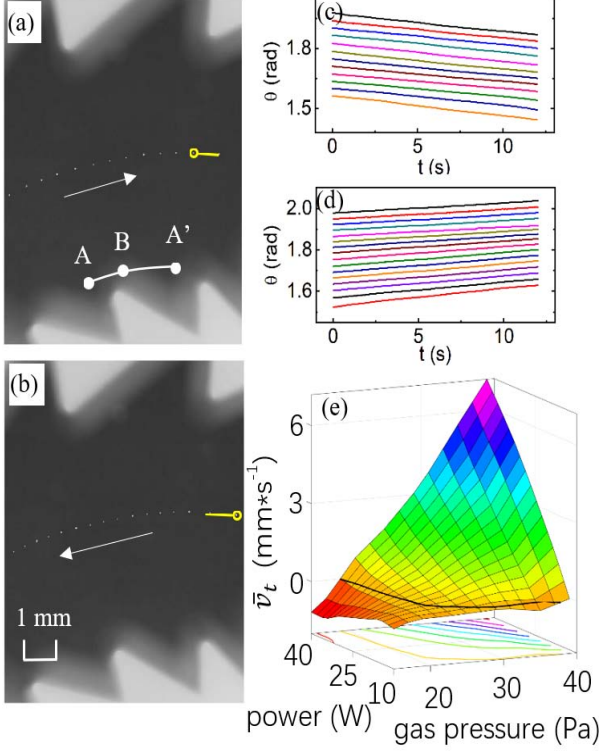


FIG. 2. (color online). Snapshots of dust particles in the negative (a) and positive (b) flows of dust particles, indicated by arrows, in the same gear structure, for the experiment conditions of (35 Pa, 10 W, peak-to-peak voltage $V_{pp} = 41$ V, dc-bias voltage $V_{dc} = -116$ V) and (40 Pa, 10 W, $V_{pp} = 39$ V, $V_{dc} = -112$ V), respectively. Typical trajectories of one selected dust particle during 12 seconds is shown by using the solid line with a starting point marked as a circle. The labels “A”, “B”, and “A’” in (a) mark the positions of the maximum, minimum, and maximum of electric potential in the arc (radius r and length $l = r\Theta$), respectively. The angular positions of dust particles (c, d) for the negative and positive flows of dust particles. (e): The mean tangential velocity \bar{v}_t of the directional motion as functions of the gas pressure and the input power. The critical line of $\bar{v}_t = 0$ is indicated by the black solid line in the surface plot. The total number of dust particles in this experiment is $N = 204$.

As our main result of this letter, we observe the steady directional motion of dust particles along the saw channel in our experiment, as shown in Fig. 2 and Supplemental Material [24]. When these dust particles are introduced into the plasma, due to their Coulomb repulsion, they arrange themselves into a circular chain along the center of the saw channel first. After about several seconds, the

circular chain of the dust particles rotates persistently along the saw channel, in the direction indicated in Fig. 2. The rotation speed of dust particles can be much higher than the thermal motion of dust particles. Our experiment here clearly demonstrates that our dusty plasma ratchet realizes the rectification of particles in plasmas.

Remarkably, we discover that the direction of the steady motion can be modified by changing the experimental conditions as shown in Figs. 2(a)-2(d). We experimentally realize both negative and positive flows of dust particles by changing the plasma conditions only as shown in Fig. 2(e). These experiment results clearly demonstrate that, in dusty plasmas, one can achieve bidirectional rectification without changing the symmetry of the sawtooth. Note that, in our experiment, the rotation speed of the dust particle chain can be modified by the plasma conditions, the gears parameter, and the number of dust particles, as we present one by one next.

Figure 2(e) illustrates the behavior of our dusty plasma ratchet with 204 dust particles, over a wide range of plasma conditions. The directional motion of the particle chain is described using the mean tangential velocities \bar{v}_t . It can be seen that, at larger gas pressure and higher input power, the mean velocity of the directional motion can be as high as ≈ 7 mm/s, with the corresponding rotation period of the dust chain is ≈ 14 s, for the plasma conditions of 40 Pa and 40 W. In Fig. 2(e), we draw a black solid line indicating the separation of the negative and positive flows of dust particles. When we set the gas pressure/input power around the critical line, the dust particles stop the directional motion and only oscillate around their equilibrium positions in the saw channel. From our observation, the transition between the negative and positive flows of dust particles is reversible by changing the gas pressure/input power.

Next we experimentally verify two keys to the rectification of dust particles: asymmetric ratchet potential and collective effect.

Asymmetric ratchet potential. —The asymmetry of the sawtooth plays one key role in the dust particle rectification. Around the gears of our experiments, the distribution of electric potential exhibits asymmetry along the saw channel (tangential direction). To illustrate the asymmetric electric potential in plasmas, a segment of arc with the radius r and length $l = r\Theta$ ($\Theta = 2\pi/n$, $n = 24$ is the number of sawtooth of the gear) is drawn in Fig. 2(a). Obviously, the electric potentials at points “A” and “A’” are higher than that at point “B”, since “B” is more close to the sheath of the inner gear. Moreover, the distribution of the electric potential along the arc is not symmetrical because of the length $l_{AB} < l_{BA'}$. This leads to an asymmetric ratchet potential, as we verify in the Supplemental Material [22].

To further confirm the key role of asymmetric ratchet potential in the rectification of dust particles, we flip the gears up-down as in Fig. 1(d), and we find that, under the

same gas pressure/input power, the direction of particle flow reverses, and the rotation speed is very similar for similar number of dust particles inside the saw channel. We also verify that symmetrical gears, as in Fig. 1(c), would not cause any net flow of dust particles for any tried plasma conditions or particle numbers.

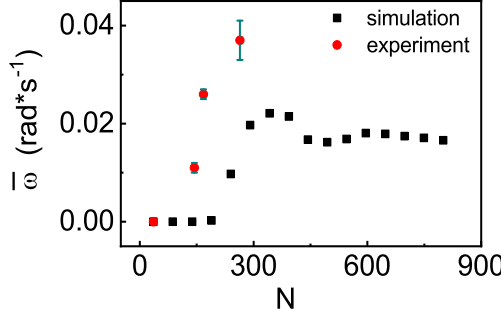


FIG. 3. The dependence of the mean angular speed on the total number of dust particles. Before the formation of multilayers of dust particles inside the saw channel, N less than about 300, the mean angular speed increases from zero with the total number of dust particles in both experiments and simulations at 45 Pa, 11 W, $V_{pp} = 45$ V, $V_{dc} = -108$ V.

Collective effect. —The collective effect of the interparticle interaction plays the other key role in the rectification of these charged dust particles. When the number of dust particles is too small, we do not observe directional flow of dust particles, i.e., the mean angular speed $\bar{\omega} = \sum_{i=1}^N \omega_i / N = 0$ rad/s, as shown in Fig. 3. At this moment, these dust particles are just trapped inside the ratchet potential. When the number of dust particles increases until the chain of dust particles forms and occupies the whole saw channel, the collective effect works, and the directional flow of dust particles occurs. The mean angular speed increases with the number of dust particles as shown in Fig. 3.

However, in our experiments, more than about 300 introduced dust particles will cause multilayers of dust particles inside the saw channel. As a result, the ion wake effect in the plasma sheath [18, 25] would substantially modify the dynamics of dust particles. Here, we only focus on the dynamics of a single layer of dust particles. The maximum angular speed obtained is $\bar{\omega} = 0.037$ rad/s, when the number of dust particles is $N \sim 266$.

The collective effect of the particle repulsion was also found in the organic electronic ratchet [26] and the superconducting ratchet [27]. In our case, the dust particles are strongly coupled due to their high charges $Q \sim -9.5 \times 10^4 e$ (typical value from simulations [22], where e is the elementary charge), which is close to that calculated from empirical formula $Q = -1400r_d T_e e \sim -6.9 \times 10^4 e$ [28]. The high charges of dust particles are capable of enhancing this collective effect to speed up the

flow of dust particles.

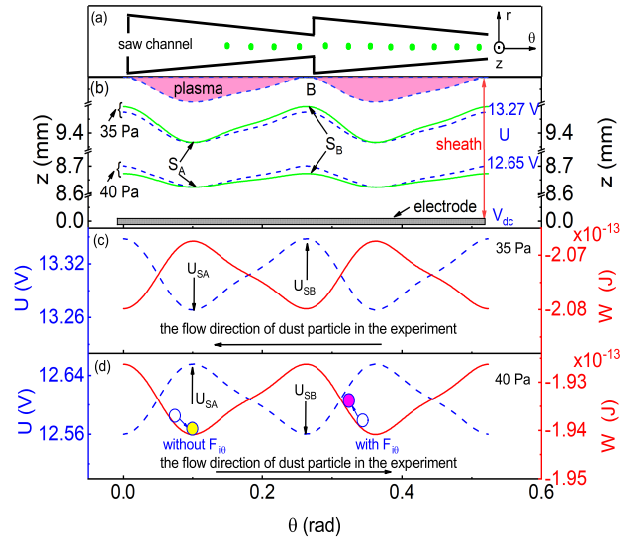


FIG. 4. (color online). (a): Diagram of the saw channel within two sawteeth. Points indicate the dust particles. (b): Balance heights of dust particles above the lower electrode (solid lines in which $mg = -Q \frac{\partial U}{\partial z}$, where U is the electric potential) and isoelectric potential lines (dashed lines) of $U=12.65$ and 13.27 V in the sheath, at 35 and 40 Pa, from COMSOL simulations. The solid lines of balance position don't overlap with the dashed isoelectric potential lines, which means that the electric potential in the balance position is variable. (c)-(d): Electric potential U (dashed line) and electric potential energy $W = QU$ (solid line) in the balance height [solid line in (b)] of dust particles at 35 and 40 Pa. The orientation of the asymmetry of electric potential energy at 35 Pa is opposite to that at 40 Pa, which results in the reversal of particle flow. (d) also illustrates how a single particle moves from initial position (hollow circle) to steady position (filled circle) without/with the ion drag force $F_{i\theta}$ in the potential well. (c): $V_{pp} = 41$ V, $V_{dc} = -116$ V, $n_{e,i} \sim 1.1 \times 10^{15} \text{ m}^{-3}$, $T_e \sim 4.4$ eV. (d): $V_{pp} = 39$ V, $V_{dc} = -112$ V, $n_{e,i} \sim 1.5 \times 10^{15} \text{ m}^{-3}$, $T_e \sim 4.3$ eV. Plasma power: 10 W.

Numerical simulations. —Firstly, we obtain the plasma parameters such as the electric potential inside the whole saw channel by using COMSOL simulations [22, 29]. Next, we consider the confinement to the charged dust particle in r -, z -, and θ - directions as defined in Fig. 4(a), respectively. In the radial r - direction, dust particle is confined around the center of the saw channel by the gears, as indicated by the points in Fig. 4(a), which agrees with the experimental trajectories [Figs. 2(a) and 2(b)]. In the vertical z - direction, the thickness of the sheath changes periodically with the width of the saw channel [30]. Therefore, the balance height of dust particle in the sheath of the lower electrode, at where $mg = -Q \frac{\partial U}{\partial z}$ (U is the electric potential), follows a wavy line as illustrated

by the solid line in Fig. 4(b). The dust particles would flow along this wavy line under an azimuthal θ - driving as illustrated below.

We find that the solid wavy lines of balance height don't overlap with the dashed isoelectric potential lines in the sheath at 35 Pa and 40 Pa as indicated in Fig. 4(b). This is reasonable because the balance height is determined by the vertical potential gradient $\frac{\partial U}{\partial z}$, not by U . Therefore, the electric potential in the solid wavy line is variable. Figure 4(c) shows the electric potential U (energy $W = QU$) along the solid wavy line of the balance height in Fig. 4(b) at 35 Pa. It exhibits a ratchet potential with clear asymmetry within each sawtooth, and the electric potential U_{SB} at S_B is larger than U_{SA} at S_A . Under the driving of a non-zero net ion drag force as shown below, the negatively-charged dust particles flow along the slanted side across the potential barrier to the next steep side of potential well, thus, the negative flow of dust particles is achieved.

However, at 40 Pa as shown in Fig. 4(d), the electric potential U_{SB} is smaller than U_{SA} , which results in that the asymmetric orientation of the ratchet potential reverses as compared with the case of 35 Pa. This leads to the positive flow of dust particles. Therefore, the reversal of particle flow essentially originates from the reversal of the asymmetric orientation of the ratchet potential at different gas pressures.

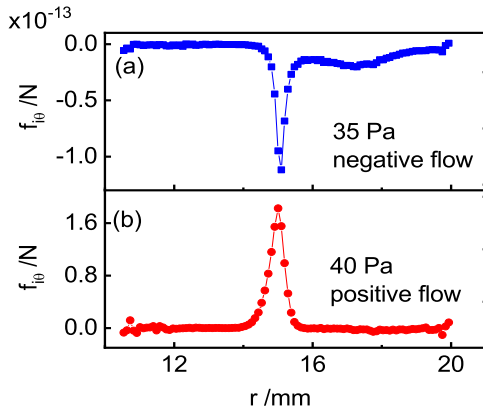


FIG. 5. (color online). Radial distribution of net ion drag force. $f_{i\theta}(r) < 0$ ($f_{i\theta}(r) > 0$) leads to the negative (positive) flow of the dust particles. The peaks of curves appear around the center of the saw channel at $r_c \approx 15.1$ mm, at where the dust particles distributed. Parameters are the same as that in Figs. 4(c) and 4(d).

For a single dust particle without the azimuthal ion drag, $F_{i\theta}=0$, it will necessarily relax to the potential well minimum position from a stochastic initial position (hollow circle) [Fig. 4(d)]. However, in the present of ion drag, it is pushed away from the potential well minimum position to somewhere on the slope of the potential well.

When a particle chain forms (collective effect works), with the help from other particles via interparticle repulsion, a dust particle could climb more easily over the potential barrier along the slanted side rather than the steep side of the potential well, which results in persistent particle flow. In order to characterize the collective effect of particle chain, we define a net ion drag force as $f_{i\theta}(r) = \frac{\oint_{l(r)} \mathbf{F}_{i\theta}(r) \cdot d\mathbf{l}(r)}{l(r)}$, a circulation of the azimuthal ion drag force divided by the circular path of integration $l(r)$. Due to the asymmetry of ratchet potential, this net ion drag force could be non-zero and $f_{i\theta}(r) < 0$ ($f_{i\theta}(r) > 0$) results in the negative (positive) flow of the particle chain [Fig. 5]. This non-equilibrium driving force of ion drag is in the order of $\sim 10^{-13}$ N, which could overcome the drag force from the neutral gas about $\sim 10^{-13}$ N to generate steady directional flow of dust particles.

Based on the above analyses, we also perform numerical simulations of dust particles, with the four forces acting on dust particles of the interparticle Yukawa interaction, the electric force, the neutral gas damping, as well as the driving from ion drag, as described in details in [22]. We obtain both negative and positive flows of dust particles by combining the asymmetric ratchet potential with the collective effect, well consistent with our experiments. We also find that when the number of dust particles is more than 340, the directional motion of dust particles decreases with the dust particle number, as shown in Fig. 3. We speculate that too dense dust particles would consume too much kinetic energy of the directed motion from this dusty plasma ratchet, so that the kinetic energy per dust particle is reduced somehow.

Summary – We demonstrate the flow rectification of dust particles in a dusty plasma experiment and the manipulation of the direction of particle flow by changing the plasma conditions of the gas pressure or the plasma power. We also perform numerical simulations by combining the COMSOL of plasma parameters with the equation of motion of dust particles to verify our experiments. We verify that the asymmetric electric potential and the collective effect play the key roles in the flow rectification of this dusty plasma ratchet.

For two particle species suspended at different height in the saw channel, the asymmetric orientation of the respective electric potential energy could reverses even at the same control parameters [22], which opens new possibility of steering different particle species in opposite directions. This dusty plasma ratchet model can operate at wider plasma density, $\sim 10^{11}\text{-}10^{16}$ m⁻³ as we tested, which means that the energy harvest of dust particles from plasma via rectification mechanism could be applied in more extensive fields.

This work is supported by the National Natural Science Foundation of China (Grant No. 11975089), the Program for National Defense Science and Technology Innovation Special Zone, the Program for Young Top-Notch

Talents of Hebei Province, and the GDUPS (2016). Work in Suzhou is supported by the National Natural Science Foundation of China under Grant No. 11875199 and the 1000 Youth Talents Plan.

[1] G. E. Morfill and A. V. Ivlev, *Rev. Mod. Phys.* **81**, 1353 (2009).

[2] P. K. Shukla and B. Eliasson, *Rev. Mod. Phys.* **81**, 25 (2009).

[3] J. H. Chu and Lin. I, *Phys. Rev. Lett.* **72**, 4009 (1994).

[4] M. Rubin-Zuzic, G. E. Morfill, A. V. Ivlev, R. Pompl, B. A. Klumov, W. Bunk, H. M. Thomas, H. Rothermel, O. Havnes, and A. Fouqué, *Nature Physics* **2**, 181 (2006).

[5] A. A. Mamun, P. K. Shukla, and G. E. Morfill, *Phys. Rev. Lett.* **92**, 095005 (2004).

[6] G. Kalman, M. Rosenberg, and H. E. DeWitt, *Phys. Rev. Lett.* **84**, 6030 (2000).

[7] T. Ott, M. Bonitz, P. Hartmann, and Z. Donkó, *Phys. Rev. E* **95**, 013209 (2017).

[8] Y. N. Wang, L. J. Hou, and X. G. Wang, *Phys. Rev. Lett.* **89**, 155001 (2002).

[9] C. Killer, T. Bockwoldt, S. Schütt, M. Himpel, A. Melzer, and A. Piel, *Phys. Rev. Lett.* **116**, 115002 (2016).

[10] H. M. Thomas and G. E. Morfill, *Nature* **379**, 806 (1996).

[11] C. S. Wong, J. Goree, Z. Haralson, and B. Liu, *Nature Physics* **14**, 21 (2017).

[12] E. Thomas Jr, U. Konopka, R. L. Merlino, and M. Rosenberg, *Phys. Plasmas*, **23**, 055701 (2016).

[13] A. Douglass, V. Land, K. Qiao, L. Matthews, and T. Hyde, *Phys. Plasmas* **19**, 013707 (2012).

[14] D. P. Resendes, G. Sorasio, and P. K. Shukla, *Physica Scripta* **T98**, 87 (2002).

[15] P. Hartmann, A. Douglass, J. C. Reyes, L. S. Matthews, T. W. Hyde, A. Kovács, and Z. Donkó, *Phys. Rev. Lett.* **105**, 115004 (2010).

[16] Y. Feng, J. Goree, and B. Liu, *Phys. Rev. Lett.* **105**, 025002 (2010).

[17] G. Joyce, M. Lampe, and G. Ganguli, *Phys. Rev. Lett.* **88**, 095006 (2002).

[18] A. Melzer, V. A. Schweigert, and A. Piel, *Phys. Rev. Lett.* **83**, 3194 (1996).

[19] A. V. Ivlev, U. Konopka, and G. E. Morfill, *Phys. Rev. E* **68**, 026405 (2003).

[20] R. P. Feynman, R. B. Leighton, and M. Sands, *The Feynman Lectures on Physics* (Addison-Wesley, Reading, MA), Vol. I. (1963).

[21] P. Hänggi and F. Marchesoni, *Rev. Mod. Phys.* **81**, 387 (2009).

[22] See Supplemental Material for a detailed description of setup, a experimental confirmation of the ratchet potential, a brief description of the COMSOL model, and expressions of the forces acting on dust particle considerd here.

[23] Y. Feng, J. Goree, and B. Liu, *Rev. Sci. Instrum.* **82**, 053707 (2011).

[24] See Supplemental Material of Videos for negative [Fig. 2(a)] and positive [Fig. 2(b)] flows of dust particles in experiments.

[25] A. Piel, *Phys. Plasmas* **24**, 033712 (2017).

[26] E. M. Roeling, W. C. Germs, B. Smalbrugge, E. J. Geluk, T. de Vries, R. A. J. Janssen, and M. Kemerink, *Nat. Mat.* **10**, 51 (2011).

[27] C. C. de S. Silva, J. Van de Vondel, M. Morelle, and V. V. Moshchalkov, *Nature* **440**, 651 (2006).

[28] M. Bonitz, C. Henning, and D. Block, *Rep. Prog. Phys.* **73**, 066501 (2010).

[29] COMSOL Multiphysics version 5.3a, www.comsol.com.

[30] D. Kim and D. J. Economou, *J. Appl. Phys.* **94**, 3740 (2003).